

A CO₂ titration electrode

Part I: Theoretical description

W. J. ALBERY, M. UTTAMLAL

Molecular Sensors Unit, The New Chemistry Laboratory, South Parks Road, Oxford OX1 3QT, Great Britain

Received 5 February 1993; revised 4 May 1993

A novel titration electrode for measuring the concentration of CO₂ is described in which OH⁻ is generated electrochemically and the time taken for the OH⁻ to be titrated by the CO₂ is measured. A theoretical description of the variation of pH with time is presented. The curve is shown to have two inflection points. The pH at the second point of inflection is close to 8. Hence the time to the second point of inflection is the titration time. Results from experiments with known quantities of OH⁻ are shown to be in good agreement with the theory.

List of symbols

a	[CO ₂]
a_{∞}	[CO ₂] in external phase
b	[HCO ₃ ⁻]
b_{∞}	[HCO ₃ ⁻] at end of titration
c	[CO ₃ ²⁻]
D_M	diffusion coefficient of CO ₂ in membrane
g	$d \ln(h)/d\tau$
h	[H ⁺]
h_0	[H ⁺] at start of titration
h_{∞}	[H ⁺] at end of titration
$h_{\max 1}$	[H ⁺] at first maximum
$h_{\max 2}$	[H ⁺] at second maximum
h_{\min}	[H ⁺] at minimum
j	flux of CO ₂ through membrane
j_0	initial flux of CO ₂ through membrane
k_0	zero order rate constant for hydration of CO ₂
k_1	first order rate constant for hydration of CO ₂

K_1	dissociation constant of H ₂ CO ₃
K_2	dissociation constant of HCO ₃ ⁻
K_H	Henry's law constant for CO ₂
K_M	partition coefficient of CO ₂ in membrane
K_W	ionisation constant for water
L	thickness of electrolyte layer
L_M	thickness of membrane
n	[Na ⁺]
r	$= k_1 K_W / k_0$
t	time
t'	$= t + t_{\max 2} - 2t_{\max 1}$
t_g	generation time
t_t	titration time
$t_{\max 1}$	time to first maximum
$t_{\max 2}$	time to second maximum
τ	$= t/t_t$
$\tau_{\max 1}$	value of τ at first maximum
$\tau_{\max 2}$	value of τ at second maximum
τ_{\min}	value of τ at minimum

1. Introduction

These three papers describe the development of a novel titration electrode for the measurement of CO₂. The electrode is similar to a Clark oxygen electrode [1] except that behind the membrane, as shown in Fig. 1 there is a more complicated electrode arrangement. The electrode works by generating a known amount of OH⁻ at constant current on the generating electrode for a time t_g . At the end of the generation phase, the titration of the OH⁻ by CO₂ diffusing through the membrane is followed potentiometrically by the indicator electrode, which is made of iridium oxide. The titration is complete when the emf/time curve passes through a point of inflexion near pH 7: the time to reach this point, t_t , is measured. The concentration of CO₂ outside the membrane is proportional to t_g/t_t . The new sensor has an excellent dynamic range and can be used to measure concentrations of CO₂ from ambient to one atmosphere. A further advantage is that the sensor is self-calibrating

from the point of inflexion. The concentration is found by measuring two times; the electrode need not obey the Nernst equation. In this paper we present a theoretical description of the e.m.f./time curve during the titration. Experimental results are shown to be in good agreement with the theory. Covington and co-workers have studied potentiometric titrations of the carbonate/hydroxide system [2-5], but there is a difference between adding H⁺ at a constant rate to a mixture of carbonate and hydroxide (the Covington system) and adding carbon dioxide at a constant rate to hydroxide ion (our system). In these experiments we used a glass electrode to measure pH rather than the iridium oxide electrode used in the sensor. In part 2[6] we describe the practical development of the sensor, present calibration plots and describe the application of the sensor to measuring CO₂ in glasshouses. In a third paper [7] we describe the application of this sensor together with sensors for glucose and oxygen to the online monitoring of the fermentation of beer.

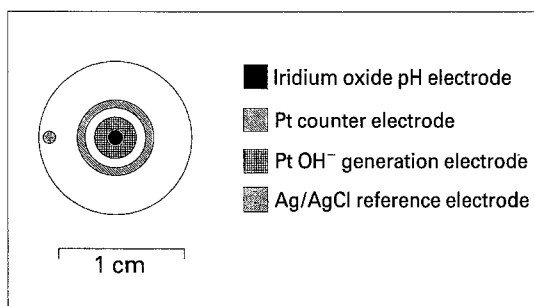
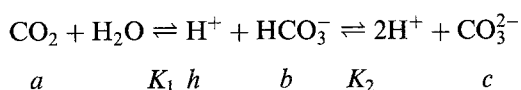


Fig. 1. Diagram of titration electrode assembly.

2. Theoretical description

In the CO₂/OH⁻ system the following equilibria will be present:



where a , h , b and c are the concentrations of the respective species.

The flux j of CO₂ through the membrane is given by

$$j = \frac{d(a+b+c)}{dt} = j_0(1 - a/a_\infty) \quad (1)$$

where for the sensor

$$j_0 = D_M K_M a_\infty / (L_M L) \quad (2)$$

and a_∞ is the concentration of CO₂ in the external medium if it is aqueous. For an external gas phase, $a_\infty = K_H p$, where K_H is the Henry's law constant and p is the partial pressure of CO₂. At the start of the titration

$$a + b + c = 0 \quad (3)$$

and

$$n = [\text{OH}^-]_0 = K_W/h_0 \quad (4)$$

where n is [Na⁺]. In the experiments described in this paper CO₂ was bubbled through the solution, and as discussed below, j_0 is controlled by the kinetics of the hydration of CO₂.

Assuming that at the start $h \ll [\text{OH}^-]$, electroneutrality requires that throughout the titration

$$h + K_W/h_0 = b + 2c + K_W/h \quad (5)$$

Using

$$c = K_2 b/h \quad (6)$$

we then find that

$$b = (h + K_W/h_0 - K_W/h)/(1 + 2K_2/h) \quad (7)$$

and

$$a = hb/K_1 \quad (8)$$

Substitution of Equation 7 in Equations 6 and 8,

followed by differentiation gives

$$\frac{da}{dt} = \left[\frac{n(1 + 4K_2/h) + h(2 + 6K_2/h) - 2K_2 K_W/h^2}{K_1(1 + 2K_2/h)^2} \right] \times \frac{dh}{dt} \quad (9)$$

and

$$\frac{dc}{dt} = \left\{ \frac{(K_2/h^2)[2K_2 - n + (K_W/h)(2 + 2K_2/h)]}{(1 + 2K_2/h)^2} \right\} \frac{dh}{dt} \quad (10)$$

Differentiation of Equation 5 gives

$$\frac{db}{dt} = (1 + K_W/h^2) \frac{dh}{dt} - 2 \frac{dc}{dt} \quad (11)$$

Towards the end of the titration the electroneutrality condition means that $b_\infty \approx n$. This clamping of the concentration of HCO₃⁻ in turn leads to

$$a/a_\infty \approx h/h_\infty \quad (12)$$

Combining Equations 1, 9, 10, 11 and 12 we obtain

$$f(h) \frac{d \ln(h)}{d\tau} = (1 - h/h_\infty) \approx 1 \quad (13)$$

where

$$\tau = t j_0 / n = t/t_t \quad (14)$$

and

$$\begin{aligned} f(h) = & [(h/K_1)(2h + n + 6K_2) + 4K_2 n/K_1 \\ & + (K_2/h)(n - 2K_2 - 2K_W/K_1) \\ & - (2K_2 K_W/h^2)(1 + K_2/h)] / [n(1 + 2K_2/h)^2] \\ & + \frac{h}{n} + \frac{K_W}{hn} \end{aligned} \quad (15)$$

The approximation in Equation 13 is justified because we shall show below that the titration is completed at the second maximum where $h \ll h_\infty$. Now in Equation 15 $n \sim 10^{-3} \text{ mol dm}^{-3}$ while $h < 10^{-6} \text{ mol dm}^{-3}$, $K_2 \sim 10^{-10} \text{ mol dm}^{-3}$ and $K_W/K_1 \sim 10^{-7} \text{ mol dm}^{-3}$. These values allow us to simplify the equation:

$$\begin{aligned} f(h) = & \frac{h/K_1 + 4K_2/K_1 + K_2/h - (2K_2 h_0/h^2)(1 + K_2/h)}{(1 + 2K_2/h)^2} \\ & + \frac{h_0}{h} \end{aligned}$$

Neglecting a term $4K_2/K_1$ compared to unity, this equation may be rearranged to give

$$f(h) = \frac{h}{K_1} + \frac{h(h_0/2 + K_2)}{(h + 2K_2)^2} + \frac{h_0}{2h} \quad (16)$$

The rate of change of pH with time is proportional to the reciprocal of $f(h)$. We will now show that this rate passes through a first maximum followed by a minimum and then a second maximum. This means that the emf time curve has three points of inflexion.

Differentiating Equation 16 we find

$$\frac{df(h)}{dh} = \frac{1}{K_1} + \frac{(h_0 + 2K_2)(K_2 - h/2)}{(h + 2K_2)^3} - \frac{h_0}{2h^2} \quad (17)$$

At the start of the titration h is usually much smaller than K_2 . Under these conditions the dominant terms in Equation 17 are the K_2 term and the third term. We then find that $f(h)$ passes through a minimum or dE/dt through a maximum when

$$h_{\max 1} = (2K_2 h_0)^{1/2} \quad (18)$$

Later on as h approaches K_2 , the second term in Equation 17 becomes the dominant term and $f(h)$ passes through a maximum or dE/dt through a minimum when

$$h_{\min} = 2K_2 \quad (19)$$

Finally at the end of the titration $h \gg K_2$. The dominant terms in Equation 17 are now the first term and the h part of the second term. We then obtain the condition for the second minimum in $f(h)$ or the second maximum in dE/dt :

$$h_{\max 2} = (K_1 K_2)^{1/2} \quad (20)$$

From Equations 13 and 16 we obtain

$$d\tau = \left[\frac{1}{K_1} + \frac{K_2}{(h + 2K_2)^2} + \frac{h_0}{2h^2} \right] dh \quad (21)$$

Integration then gives

$$\tau = \left(1 - \frac{h_0}{h} \right) \left[\frac{h}{K_1} + \frac{h}{2h + 4K_2} + \frac{1}{2} \right] \quad (22)$$

We then find that the time to the first maximum when $h_0 \ll h \ll K_2$ is given by

$$\tau_{\max 1} = 1/2 \quad (23)$$

At the minimum from Equation 19, $h_{\min} = 2K_2$ and from Equation 22

$$\tau_{\min} = 3/4 \quad (24)$$

At the second maximum when $h_{\max 2} = (K_1/K_2)^{1/2}$ both the K_1 and K_2 terms in Equation 22 are much less than 1 and we find

$$\tau_{\max 2} = 1 \quad (25)$$

From Equations 16, 18, 19 and 21 we find the following values for $f(h)$:

$$f(h)_{\max 1} = (h_0/2K_2)^{1/2} \ll 1 \quad (26)$$

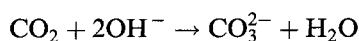
$$f(h)_{\min} = 1/8 \quad (27)$$

and

$$f(h)_{\max 2} = 2(K_2/K_1)^{1/2} \ll 1 \quad (28)$$

Remember that dE/dt is proportional to the reciprocal of $f(h)$.

The reason for the results in Equations 23 to 28 is that during the first phase of the titration, $\tau \leq 1/2$. The overall reaction is



Because of the logarithmic pH scale dE/dt increases as this titration proceeds. In the second phase when $\tau \sim 3/4$ the pH is close to $\text{p}K_2$ and the main reaction is



The buffering action of the K_2 equilibrium slows down the rate of change of the pH going through a minimum at $h = 2K_2$. Beyond the minimum the diminishing concentration of CO_3^{2-} and the logarithmic scale means that dE/dt increases again. With a constant flux of CO_2 it takes an equal amount of time to form the CO_3^{2-} and then to destroy it again. Hence the maxima occur at $\tau = 1/2$ and $\tau = 1$; by the end of the titration each CO_2 molecule has consumed one OH^- to make HCO_3^- .

Inspection shows that Equation 22 is an intractable cubic equation relating h to τ . However for $\tau < 0.75$, where $\tau = 0.75$ corresponds to the minimum in $d\ln(h)/d\tau$, the h^3 term is negligible compared to the other three terms. The resulting quadratic equation then gives

$$h = \frac{1}{2(1-\tau)} \times \{ [K_2(1-\tau) - h_0]^2 + 4K_2h_0(1-\tau) \}^{1/2} - K_2(1-2\tau) + h_0 \} \quad (29)$$

Conversely for $\tau > 0.75$ the h^0 term is negligible compared to the other three terms and the resulting quadratic equation then gives

$$h = \frac{1}{2} \{ [K_1(1-\tau)^2 + 8K_1K_2(\tau - 1/2)]^{1/2} - K_1(1-\tau) \} \quad (30)$$

Using either Equation 29 or 30 we can calculate values of h as a function of τ and hence using Equations 13 and 16 we can calculate $d\ln(h)/d\tau$ as a function of τ .

In the experiments reported in this paper we used an ordinary glass electrode and pH meter to obtain more reliable measurements of pH. CO_2 was bubbled through the reaction vessel. Under these conditions the flux, j , is controlled by the kinetics of the hydration reaction. We found that contrary to Equations 23 and 25 the time to the first maximum was always less than half the time to the second maximum. The reason for this is that the hydration reaction can be catalysed by OH^- . We therefore write

$$j_0 = k_0 + k_1[\text{OH}^-] = k_0(1 + r/h) \quad (31)$$

where k_0 and k_1 are zero and first order rate constants, respectively, and

$$r = k_1K_W/k_0 \quad (32)$$

In Equation 21 we select the two terms that are important at high pH and modify the expression to take account of Equation 31:

$$d\tau = \frac{1/4K_2 + h_0/2h^2}{1 + r/h} dh \quad (33)$$

Writing $d\ln(h)/d\tau$ as g , we can solve the quadratic

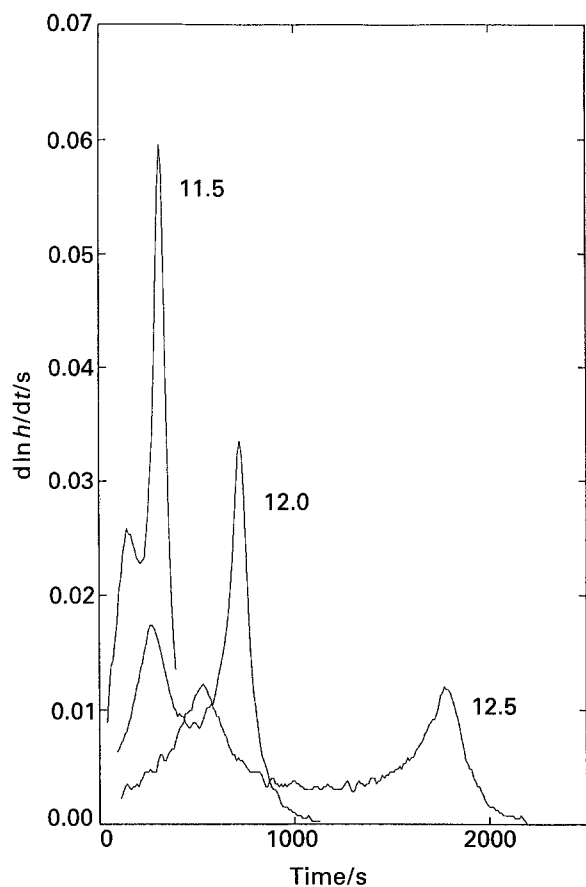


Fig. 2. Typical traces of $d \ln(h)/dt$ against time. In this and subsequent figures each trace is labelled with the initial pH. For the experiments in this figure and in subsequent figures there was no added background electrolyte.

equation to obtain

$$h = \frac{2K_2}{g} \left\{ 1 - \left[1 - \frac{g}{K_2} \left(\frac{gh}{2} - r \right) \right]^{1/2} \right\} \quad (34)$$

Equation 33 can be integrated to give:

$$\frac{h - h_0}{4K_2} + \frac{h_0}{2r} \ln(h/h_0) - \left[\frac{r}{4K_2} + \frac{h_0}{2r} \right] \ln \left[\frac{h+r}{h_0+r} \right] = \tau \quad (35)$$

This pair of equations relate g and τ for $\text{pH} > 11$.

3. Experimental details

To verify the theoretical model with more precise measurements of h , a standard glass electrode and pH meter were used (Corning pH meter 245). The initial pH was achieved by adding NaOH solution to NaCl electrolyte of varying concentrations. A 5 cm³ sample was transferred to a 6 cm³ beaker through which 5% CO₂/95% O₂ supplied by BOC Ltd was bubbled at a volumetric flow rate of 75 cm³ min⁻¹. All other chemicals were of AnalaR grade. The pH time data were acquired at ten second intervals and stored in an Amstrad 1512 microcomputer.

4. Results and discussion

In fitting a calculated curve to experimental data we

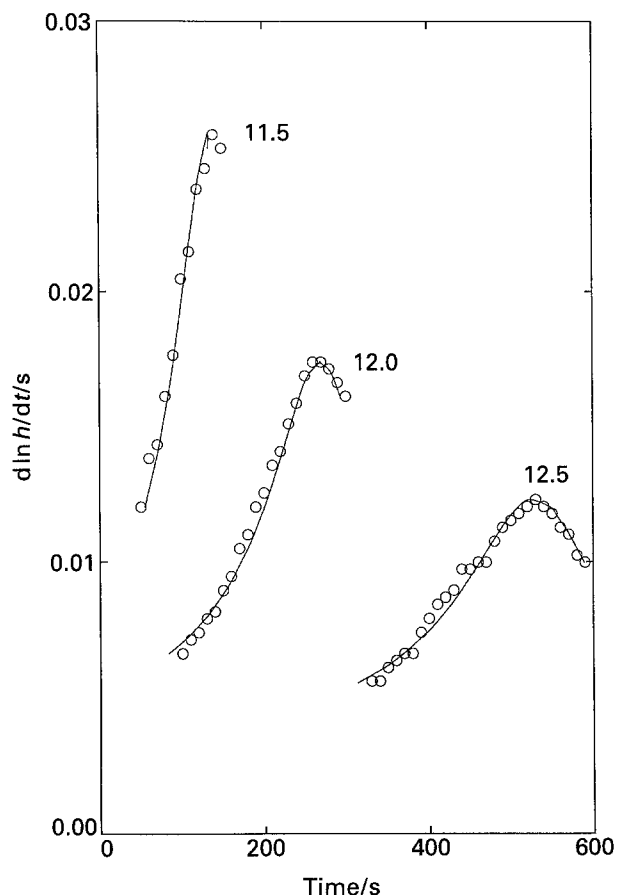


Fig. 3. Typical fit of experimental data (points) to calculated curves from Equations 34 and 35 for data before the first maximum.

first convert pH to $\ln(h)$:

$$\ln(h) = -2.303(\text{pH})$$

and then differentiate using Lagrange's three-point formula [4] to obtain values of $d \ln(h)/dt$ as a function of t . The shape of this curve depends on five parameters, h_0 , r , K_1 , K_2 and t_i . In each case we found as predicted two maxima and a minimum. Typical results are displayed in Fig. 2. As required by Equations 23 to 25 the time of the minimum was half way between those of the two maxima. The analysis takes place in three parts. First we use Equations 34 and 35 to analyse the data at high pH before the first maximum. We know h_0 and from this analysis we obtain values for r and K_2 . Secondly we use the data between the first maximum and the minimum ($0.5 < \tau < 0.75$) and Equation 29 to find values of K_2 and t_i . Finally we use the data beyond the minimum and Equation 29 to find values of K_1/K_2 and t_i . The calculations were performed using Sigmaplot 4.1. Because the OH⁻ catalysis described by r means that the time to the first maximum is less than half the time to the second maximum we use a corrected time scale, t' , between the two maxima by writing

$$t' = t + t_{\text{max}2} - 2t_{\text{max}1} \quad (36)$$

Typical fits of the experimental data to theoretical curves are displayed in Figs 3 to 5. Satisfactory fits are found in all cases.

From the data before the first maximum we find the

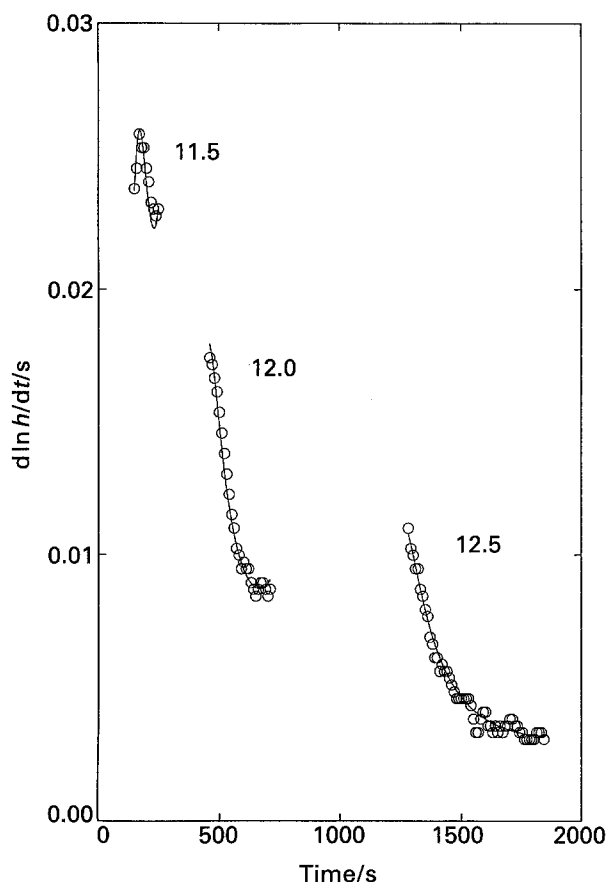


Fig. 4. Typical fit of experimental data (points) to calculated curves from Equations 13 and 29 for data between the first maximum and the minimum.

values of r and K_2 reported in Tables 1 and 2. At the lower ionic strengths the values of r are roughly constant. This we would expect since there will not be a large kinetic salt effect on either k_0 or k_1 . From the data between the first maximum and minimum we find the second set of values of K_2 reported in Table 2. It is satisfactory that the results agree with those from before the maximum. The results in brackets are less precise than the remainder because the r effect continues beyond the first maximum and hence there are less data that we can use which are sensitive to the value of K_2 . From the Debye Huckel theory we would expect K_2 to increase with ionic strength as is observed; the literature value [9] at infinite dilution is 5×10^{-11} M. From the data beyond the minimum and the mean values of K_2 we find the values of K_1 reported in Table 3. The Debye Huckel theory predicts that changing the ionic strength should not affect K_1 and indeed there is no discernable trend. Averaging the data we find a value of

Table 1. Values of r/pM

$[NaCl]/M$	h_0/M	3.2×10^{-12}	10^{-12}	3.2×10^{-13}	Mean
0.00	1.0	1.4	1.0		1.1 ± 0.1
0.10	1.0	1.4	1.1		1.2 ± 0.1
0.50	1.9	1.1	1.1		1.4 ± 0.3
1.00	2.4	2.6	1.5		2.2 ± 0.3

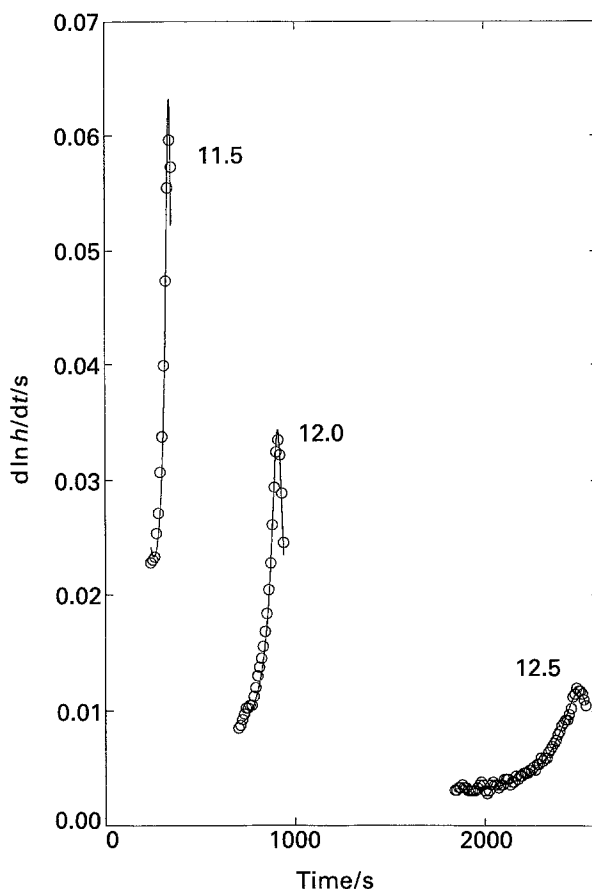


Fig. 5. Typical fit of experimental data (points) to calculated curves from Equations 16 and 30 for data between the minimum and the second maximum.

Table 2. Results for K_2/pM from before and after the first maximum

h_0/pM $[NaCl]/M$	3.16	1.00	0.316	Mean
0.00 before	96 ± 8	100 ± 3	116 ± 2	
after	84 ± 3	110 ± 2	134 ± 10	
Mean	90 ± 6	105 ± 5	125 ± 9	
0.10 before	146 ± 6	114 ± 2	146 ± 6	
after	132 ± 15	120 ± 4	161 ± 12	137 ± 8
0.50 before	206 ± 2	209 ± 6	208 ± 3	
after	165 ± 6	215 ± 4	(162 ± 37)	201 ± 9
1.00 before	324 ± 8	419 ± 14	306 ± 16	
after	368 ± 2	478 ± 17	(342 ± 33)	379 ± 31

$3.6 \pm 0.5 \times 10^{-7}$ M to be compared with a literature value of 4.5×10^{-7} M [10].

Finally we turn to the most important parameter for the titration sensor, t_t . From Equation 14.

$$t_t h_0 = K_W / j_0 \quad (38)$$

Results for $t_t h_0$ are collected in Table 4. Good agreement was found in each case for the value of t_t from the data before and after the minimum and from the time between the first and second maxima. It is also very satisfactory that in each case the same value of t_t not only successfully describes the time between the two maxima, but also, see Equation 27, describes

Table 3. Results for K_1/pM from beyond the minimum

h_0/pM [NaCl]/M	3.16	1.00	0.316	
0.00	0.15 ± 0.01	0.39 ± 0.01	0.36 ± 0.01	
0.10	0.16 ± 0.02	0.35 ± 0.01	0.30 ± 0.01	
0.50	0.30 ± 0.02	0.51 ± 0.01	0.29 ± 0.01	
1.00	—	0.77 ± 0.01	0.42 ± 0.01	

Table 4. Results for $t'h_0/snM$ before and after the minimum

h_0/pM [NaCl]/M	3.16	1.00	0.316	Mean
0.00 before	0.94	0.89	0.78	
after	1.03	0.90	0.79	0.89 ± 0.05
0.10 before	0.78	0.75	0.73	
after	0.84	0.76	0.73	0.77 ± 0.02
0.50 before	0.96	1.02	0.94	
after	1.03	1.02	0.94	0.99 ± 0.02
1.00 before	—	1.02	1.07	
after	—	1.02	1.08	1.05 ± 0.02

the value of $[d \ln(h)/dt]_{\min}$:

$$\left(\frac{d \ln(h)}{dt}\right)_{\min} = 8/t_t \quad (39)$$

Hence the pH time profile is successfully described by the theoretical model. It is satisfactory that as given by

Equation 20 the pH of the second maximum, $(K_1 K_2)^{1/2}$, is about 8 and hence we have a self calibrating electrode with the second maximum occurring at a fixed pH very close to the endpoint of the titration. The development of the sensor will be described in the next paper.

Acknowledgement

Financial support from Whitbread PLC is gratefully acknowledged.

References

- [1] L. C. Clark, *Trans. Am. Soc. Art. Int. Org.* **2** (1956) 41.
- [2] A. K. Covington, R. A. Robinson and M. Sarbar, *Anal. Chim. Acta.* **100** (1978) 367.
- [3] A. K. Covington, R. A. Robinson and M. Sarbar, *Anal. Chim. Acta.* **130** (1981) 93.
- [4] A. K. Covington, R. N. Goldberg and M. Sarbar, *Anal. Chim. Acta.* **130** (1981) 103.
- [5] A. K. Covington, *Chem. Soc. Rev.* **14** (1985) 265.
- [6] W. J. Albery, M. S. Appleton, N. J. Freeman, B. Keccakus, M. D. Neville and M. Uttamlal, *J. Appl. Electrochem.* (1993), this issue.
- [7] W. J. Albery, M. S. Appleton, T. R. D. Pragnell, M. J. Pritchard, M. Uttamlal, L. E. Fieldgate, D. R. Lawrence and F. R. Sharpe, *J. Appl. Electrochem.* (1993), submitted for publication.
- [8] M. Abramowitz and I. A. Stegun, 'Handbook of Mathematical Functions', Dover Publications, New York (1970) p. 879.
- [9] J. T. Edsall, *N. A. S. A. Spec. Publ.* **188** (1969) 15.
- [10] D. M. Kern, *J. Chem. Educ.* **37** (1960) 14.